On the Nature of Intermolecular Interactions in Nucleic Acid Base−Amino Acid Side-Chain Complexes

Ż. Czyżnikowska,*,† P. Lipkowski,† R. W. Góra,† R. Zaleśny,† and A. C. Cheng‡

Theoretical Chemistry Group, Institute of Physical and Theoretical Chemistry, Wrocław University of Technology, Wyb. Wyspiańskiego 27, 50-370 Wrocław, Poland, and Department of Molecular Structure, Amgen Inc., One Kendall Square, Building 1000, Cambridge, Massachusetts 02139

Received: May 4, 2009; Revised Manuscript Received: June 11, 2009

Twenty hydrogen-bonded complexes composed of nucleic acid base and amino acid side chain have been analyzed using *ab initio* quantum chemistry methods with the aim of gaining insights into the nature of molecular interactions in these systems. The intermolecular interaction energies were estimated using the second-order Møller−Plesset perturbation theory and coupled clusters approach with single and double excitations, while their components have been determined by means of a hybrid variational−perturbational decomposition scheme. Additionally, the topological analysis of an electron density distribution of the studied complexes has been performed. In the case of all of the studied neutral complexes, the main source of stabilization is the delocalizaction energy associated with the electron density deformation upon the interaction which contributes almost half of the total interaction energy. Furthermore, analysis of the interaction induced difference density maps of complexes containing neutral amino acid side chains reveals that the delocalization component involves the electron density changes localized in the double-hydrogen-bonded ring structures. A relatively good correlation between the sum of densities at hydrogen-bond critical points and the Hartree−Fock intermolecular interaction energy components (electrostatic, delocalization, and exchange) has been observed for the two independently considered sets of complexes, containing positively charged and neutral amino acid side chains.

Introduction

Molecular recognition of nucleic acid sequences by enzymes and regulatory proteins plays an important role in gene expression (DNA replication, transcription, and translation). Hydrogen bonding is the most specific type of interaction occurring in amino acid−nucleic acid base complexes. Water mediated hydrogen bonds and electrostatic and hydrophobic interactions also stabilize nucleic acid−protein complexes. The key role of hydrogen bonding, between amino acid side chains and the Watson−Crick base pairs, in recognition processes was confirmed by Seeman et al.[1] The authors analyzed interactions between amino acid residues and nucleic acid bases in the major and minor groove of DNA and proposed that at least two double hydrogen bonds were involved in the recognition system for a base pair.[1] Moreover, the structural analysis of several DNA−protein complexes has revealed some frequently occurring patterns, such as Asn/Gln-A or Arg-G. Since then, the recognition phenomena have been the subject of extensive research.[2−8] Understanding how proteins recognize RNA has also been the subject of many experimental studies.[9−11]

The analysis of the intermolecular interactions is much more difficult to perform on a purely theoretical basis for RNA than for DNA. This is due to the fact that the structure of ribonucleic acid is much more complicated in comparison with DNA: In the former system, we find interactions between unpaired bases in bulges or loops as well as interactions between non-Watson−Crick base pairs with multiple hydrogen bonds. It is sufficient to say that about 5000 plausible interactions were identified during the study on the sequence-specific protein−nucleic acid recognition, but only a limited set of bidentate interactions between amino acid side chains and nucleic acid bases were identified.[12] The systematic *ab initio* analysis of interactions occurring in the recognition process of a base pair by amino acids was performed by Cheng et al.[13] The authors analyzed over 20 complexes between RNA bases and amino acids with two or more hydrogen bonds involved. They concluded that the interactions involving the charged amino acid residues (Lys, Asp/Glu, and Arg) are the most favorable with regard to intermolecular interaction energy. The present study is a further step toward better understanding of the molecular recognition process, although we neglect the influence of solvent effects. Here, we investigate the nature of intermolecular interactions in nucleic acid base−amino acid side-chain complexes in conformations considered previously[13] (see Figure 1). The primary goal of the present study is to analyze the origins of stabilization of binary nucleic acid base−amino acid side-chain complexes on a quantitative basis. This type of analysis is scarcely available in the subject literature, although the interactions of nucleic acid bases with amino acids have been studied thoroughly.[14,15] One of the few exceptions is the study performed by Gu et al.[16] They characterized the structural properties of primary recognition sites of guanine in ribonuclease T1. Moreover, they analyzed electron density deformation and performed the Kitaura−Morokuma partitioning of intermolecular interaction energy (IIE).[16] The authors concluded that the electrostatic interaction energy is a decisive factor in guanine recognition by ribonuclease T1. Indeed, in all of the complexes studied by the authors, the electrostatic contribution has the largest absolute value. However, taking into account the associated exchange repulsion, the interaction energy of the

* Corresponding author. E-mail: zaneta.czyznikowska@gmail.com.
† Wrocław University of Technology.
‡ Amgen Inc.

10.1021/jp904146m CCC: $40.75
Published on Web 07/28/2009

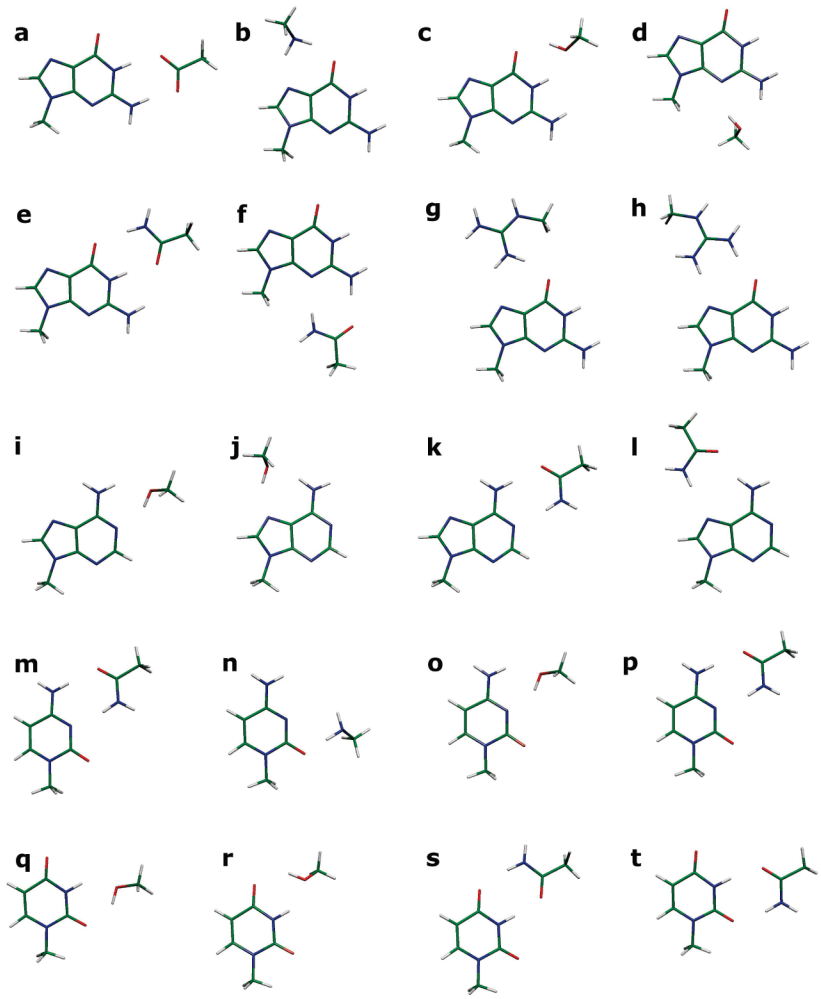

Figure 1. Nucleic acid base−amino acid side-chain complexes analyzed in the present study.

unperturbed monomer charge densities is in fact substantially smaller than the sum of polarization and charge-transfer components. As it turns out, most of the complexes studied in this work follow the same pattern. Actually, as was shown by Gutowski and Piela and later by Frey and Davidson,[17,18] the distinction between charge-transfer and polarization components loses its meaning in the complete basis set limit. Therefore, in this work, we will refer to the delocalization component instead, which is comparable to the sum of polarization and charge-transfer components obtained in the Kitaura−Morokuma scheme.[19]

Computational Details

In the present study, we analyze the results of calculations of intermolecular interaction energy and its components. In the former case, we used the supermolecular approach to compute BSSE-corrected IIEs at the MP2/aug-cc-pVDZ and CCSD/aug-cc-pVDZ levels of theory with the aid of the MOLPRO package,[20] while, in the latter case, we employed a variational−perturbational scheme as implemented in the modified version of the GAMESS US code.[21,22] Likewise, all calculations of interaction energy components were performed using the aug-cc-pVDZ basis set. More details about the variational−perturbational scheme follow in the next section.

Interaction Energy Partitioning. In this work, we have adopted the hybrid variational−perturbational approach, which retains the rigorous physical meaning and clarity of outline of the polarization approximation with the ease of estimation of the exchange effects in a variational approach.[23−27] In this scheme, the total interaction energy calculated in a supermolecular approach at the second-order Møller−Plesset perturbation theory is partitioned into the Hartree−Fock and Coulomb electron correlation interaction energy components:

$$\Delta E^{\mathrm{MP2}} = \Delta E^{\mathrm{HF}} + \epsilon^{(2)}_{\mathrm{MP}} \tag{1}$$

The Hartree−Fock interaction energy term can be partitioned into the Heitler−London interaction energy, encompassing the electrostatic interactions of unperturbed monomer charge densities as well as the associated exchange repulsion, and the $\Delta E^{\mathrm{HF}}_{\mathrm{del}}$ component encompassing collectively the induction and the associated exchange effects due to the Pauli exclusion principle, and since their separation could lead to a nonphysical charge transfer,[17,18] it is not being partitioned any further.

$$\begin{aligned}\Delta E^{\mathrm{HF}} &= \Delta E^{\mathrm{HF}}_{\mathrm{del}} + \Delta E^{\mathrm{HL}} \\ &= \Delta E^{\mathrm{HF}}_{\mathrm{del}} + \epsilon^{(10)}_{\mathrm{el}} + \epsilon^{\mathrm{HL}}_{\mathrm{ex}}\end{aligned} \tag{2}$$

The second order electron correlation correction term, $\epsilon^{(2)}_{\mathrm{MP}}$, can be decomposed into the second-order dispersion interaction and the correlation corrections to the Hartree−Fock components.[25,26]

$$\epsilon_{MP}^{(2)} = \epsilon_{disp}^{(20)} + \epsilon_{el,r}^{(12)} + \Delta E_{ex\text{-}del}^{(2)} \quad (3)$$

The $\epsilon_{el}^{(10)}$ and $\epsilon_{disp}^{(20)}$ terms are obtained in a standard polarization perturbation theory,[28] whereas the $\epsilon_{el,r}^{(12)}$ term is calculated using the formula proposed by Moszynski et al.[29] In all necessary calculations, the dimer centered basis set (DCBS) is consistently used and therefore the results are basis set superposition error (BSSE) free due to the full counterpoise correction.[30]

The detailed outline of interaction energy partitioning scheme and the recent implementation adopted in this work can also be found elsewhere.[31−33]

Interaction Difference Densities. Very helpful in interpretation of the results of interaction energy partitioning is an analysis of the interaction difference densities (IDD):

$$\Delta\rho(\mathbf{r}) = \rho_{AB}(\mathbf{r}) - \rho_{A}(\mathbf{r}) - \rho_{B}(\mathbf{r}) \quad (4)$$

which allow the changes in the electron density distributions of monomers occurring upon their interaction to be visualized. The IDD isodensity maps, presented in this study, were plotted using the electron density matrices obtained by subtraction of the one-particle density matrices of monomers (A, B) from the density matrix of dimer (AB), all corresponding to the respective Hartree−Fock solutions. Since the alterations of the electron density distributions of the interacting subsystems occurring at the Heitler−London level of theory are only due to the small rotations of orbitals, accompanying their orthogonalization, the visible changes can be attributed almost exclusively to the delocalization interaction energy term. The interaction difference density maps were plotted using the modified version[34] of the MOLDEN program.[35]

Atoms in Molecules Method. In this study, the topological features of electron density in the studied complexes shall be exploited using the quantum theory of atoms in molecules (QTAIM) of Bader.[36,37] The molecular electron density distribution $\rho(\mathbf{r})$ can be obtained from a many-particle wave function:

$$\rho(\mathbf{r}) = N\sum_{\sigma}\int\left|\Psi(\mathbf{r},\mathbf{r}_2,\ldots,\mathbf{r}_N)\right|^2 d\mathbf{r}_2,\ldots,d\mathbf{r}_N \quad (5)$$

where the summation is performed over spin coordinates and the integration is over all but one spatial coordinate and N stands for the total number of electrons. In the present study, we shall analyze both the SCF densities as well as generalized MP2 densities obtained in the Z vector approach.[38]

Particularly useful are the properties of bond critical points (BCPs) localized at the bond path linking the interacting species, especially the electronic density at BCP, $\rho(\mathbf{r}_{BCP})$, and its Laplacian, $\nabla^2\rho(\mathbf{r}_{BCP})$. Negative values of $\nabla^2\rho(\mathbf{r}_{BCP})$ imply a concentration of electronic charge in the intermolecular region. Moreover, the larger it is in magnitude, the greater the electronic charge density at BCP and the stronger the interaction energy among subsystems. Conversely, positive values of the Laplacian correspond to the depletion of electronic charge in the intermolecular region. The former case is an indication of a sharing of electronic charge density between interacting species and is commonly considered to indicate a so-called shared or a closed-shell nature of interactions.

The local kinetic $G(\mathbf{r}_{BCP})$, potential $V(\mathbf{r}_{BCP})$, and total $H(\mathbf{r}_{BCP})$ energy densities, estimated at the bond critical point, are also very helpful in analysis of the weak intermolecular interactions. The electronic energy density of the local charge distribution may be expressed as the sum of the local kinetic and potential energy densities:

$$H(\mathbf{r}_{BCP}) = G(\mathbf{r}_{BCP}) + V(\mathbf{r}_{BCP}) \quad (6)$$

The relation between the Laplacian and the components of the local energy density is given by the local expression for the virial theorem[36,39] (in atomic units):

$$\frac{1}{4}\nabla^2\rho(\mathbf{r}_{BCP}) = 2G(\mathbf{r}_{BCP}) + V(\mathbf{r}_{BCP}) \quad (7)$$

The sign of the Laplacian at a specific point in space determines whether the negative potential energy or the positive kinetic energy is in excess of the virial ratio amounting to 2. In the regions where the Laplacian is negative, the potential energy dominates, while, in the regions where its sign is positive, the kinetic energy prevails. The AIM calculations were performed using the AIM2000 program.[40]

Results and Discussion

The estimated interaction energy terms for all of the studied complexes are reported in Tables 1−4. These, however, are much easier to discuss and compare in the form of bar charts shown in Figure 2.

All of the studied systems, but one (dimer of cytosine and lysine), could be characterized as double-hydrogen-bonded complexes, although in some cases the H-bond geometry is quite far from being linear. As mentioned in the Introduction, we consider the nucleic acid base−amino acid side-chain complexes optimized at the HF/6-31G(d,p) level of theory as considered previously by Cheng et al.[13] The fact that H-bond geometries are far from being linear, however, does not seem to be the most important factor as far as the total interaction energy is concerned. The most favorable interactions were found in the complexes of guanine and cytosine with lysine where the H-bond angle is quite far from a presumably perfect linear arrangement. On the other hand, the G···Asp/Glu complex, where the H-bonds are almost linear, is about 10 kcal/mol less stable than the G···Lys. Considering the previous experimental findings[41] indicating a greater stability of H-bonds from charged side chains, it is not surprising that the most favorable interactions are observed in the negatively charged G···Asp/Glu complex and in the positively charged complexes of guanine and cytosine with lysine and arginine. In the complexes with arginine, the most significant are the electrostatic interactions. Even taking into account the exchange and correlation corrections, the Heitler−London interaction contributes almost 60% of the overall stabilization and the second most important component is the delocalization term. A similar picture of interactions can be observed in the complex of guanine and lysine. However, in the complexes of cytosine with lysine and G···Asp/Glu, this is not so obvious. The results of interaction energy partitioning indicate that, although the electrostatic interaction of the unperturbed charge densities is substantial, the stabilization due to a mutual polarization of the interacting species reflected in the large value of delocalization component is even greater and is in fact the most important contribution. In the case of all of the studied charged complexes, the Coulomb electron correlation correction is generally rather insignificant, as its contribution is always smaller than 8% of the total interaction energy.

TABLE 1: Intermolecular Interaction Energy Components for the Guanine and Amino Acid Side Chains Computed Using the aug-cc-pVDZ Basis Set[a]

complex	$\epsilon_{el}^{(10)}$	ϵ_{ex}^{HL}	ΔE_{del}^{HF}	ΔE^{HF}	$\epsilon_{el,r}^{(12)}$	$\epsilon_{disp}^{(20)}$	$\Delta E_{ex\text{-}del}^{(2)}$	$\epsilon_{MP}^{(2)}$	ΔE^{MP2}
Asp/Glu (a)	−45.87	30.70	−21.04	−36.21	0.50	−10.19	7.10	−2.59	−38.80
Lys (b)	−50.18	24.92	−19.14	−44.40	2.25	−8.07	2.98	−2.48	−47.24
Ser/Thr/Tyr (c)	−17.43	13.65	−4.98	−8.76	−0.03	−5.53	3.51	−2.14	−10.90
Ser/Thr/Tyr (d)	−14.78	13.56	−4.22	−5.40	−0.65	−6.23	3.31	−3.57	−8.97
Asn/Gln (e)	−25.89	18.03	−8.72	−16.58	1.26	−7.60	4.43	−1.91	−18.49
Asn/Gln (f)	−17.64	14.58	−5.89	−8.94	0.33	−6.94	3.47	−3.15	−12.09
Arg (g)	−36.18	16.06	−11.26	−31.38	1.68	−7.13	2.56	−2.88	−34.26
Arg (h)	−39.48	18.68	−13.88	−34.68	1.86	−7.18	2.51	−2.81	−37.50

[a] All values are given in kcal/mol.

TABLE 2: Intermolecular Interaction Energy Components for the Adenine and Amino Acid Side Chains Computed Using the aug-cc-pVDZ Basis Set[a]

complex	$\epsilon_{el}^{(10)}$	ϵ_{ex}^{HL}	ΔE_{del}^{HF}	ΔE^{HF}	$\epsilon_{el,r}^{(12)}$	$\epsilon_{disp}^{(20)}$	$\Delta E_{ex\text{-}del}^{(2)}$	$\epsilon_{MP}^{(2)}$	ΔE^{MP2}	ΔE^{CCSD}
Ser/Thr/Tyr (i)	−14.60	12.72	−4.10	−5.98	−0.65	−5.55	3.08	−3.12	−9.10	−8.49
Ser/Thr/Tyr (j)	−16.07	14.28	−4.84	−6.63	−0.70	−6.23	3.22	−3.71	−10.34	−9.51
Asn/Gln (k)	−17.05	13.49	−5.48	−9.04	−0.12	−6.10	3.18	−3.04	−12.08	−11.49
Asn/Gln (l)	−16.18	12.59	−5.16	−8.75	0.01	−5.90	2.80	−3.09	−11.85	−11.22

[a] All values are given in kcal/mol.

TABLE 3: Intermolecular Interaction Energy Components for the Cytosine and Amino Acid Side Chains Computed Using the aug-cc-pVDZ Basis Set[a]

complex	$\epsilon_{el}^{(10)}$	ϵ_{ex}^{HL}	ΔE_{del}^{HF}	ΔE^{HF}	$\epsilon_{el,r}^{(12)}$	$\epsilon_{disp}^{(20)}$	$\Delta E_{ex\text{-}del}^{(2)}$	$\epsilon_{MP}^{(2)}$	ΔE^{MP2}	ΔE^{CCSD}
Arg (m)	−37.66	17.88	−13.13	−32.91	2.23	−7.21	2.73	−2.25	−35.15	−34.76
Lys (n)	−49.40	30.20	−22.79	−42.09	3.18	−7.60	3.26	−1.16	−43.24	−43.00
Ser/Thr/Tyr (o)	−16.31	13.30	−4.71	−7.72	−0.26	−5.66	3.17	−2.75	−10.47	−9.99
Asn/Gln (p)	−21.54	15.79	−7.19	−12.95	0.54	−6.88	3.76	−2.58	−15.53	−15.04

[a] All values are given in kcal/mol.

TABLE 4: Intermolecular Interaction Energy Components for the Uracil and Amino Acid Side Chains Computed Using the aug-cc-pVDZ Basis Set[a]

complex	$\epsilon_{el}^{(10)}$	ϵ_{ex}^{HL}	ΔE_{del}^{HF}	ΔE^{HF}	$\epsilon_{el,r}^{(12)}$	$\epsilon_{disp}^{(20)}$	$\Delta E_{ex\text{-}del}^{(2)}$	$\epsilon_{MP}^{(2)}$	ΔE^{MP2}	ΔE^{CCSD}
Ser/Thr/Tyr (q)	−12.76	10.32	−3.28	−5.72	−0.13	4.64	2.56	−2.21	−7.93	−7.56
Ser/Thr/Tyr (r)	−13.54	11.04	−3.58	−6.08	−0.28	−4.81	2.82	−2.27	−8.34	−7.87
Asn/Gln (s)	−17.04	13.34	−5.78	−9.48	0.36	−5.98	3.34	−2.29	−11.77	−11.26
Asn/Gln (t)	−15.68	12.07	−5.11	−8.71	0.39	−5.70	3.05	−2.27	−10.98	−10.59

[a] All values are given in kcal/mol.

The situation is completely different in the case of the neutral complexes and especially the complexes with adenine and uracil, where the total electron correlation contribution $\epsilon_{MP}^{(2)}$ ranges from 19 to 36% of the total interaction energy. Even though the absolute value of the dispersion interaction is approximately the same as in the other studied complexes and amounts to about −6 kcal/mol, the electrostatic interaction is almost completely quenched by the Heitler−London exchange repulsion and its correlation correction, and as a result, the overall stabilization is in fact almost exclusively due to ΔE_{del}^{HF} and $\epsilon_{disp}^{(20)}$ components. Although the electron correlation correction is very important in these complexes, the MP2 level of approximation seems to be quite sufficient, at least in the case of the studied systems. In the case of neutral complexes of guanine and cytosine, there is generally greater diversity of the observed interactions. The total interaction energy in the case of most of the neutral amino acid complexes with nucleic acid bases amounts to about 10−15 kcal/mol which is only about 25% of the average interaction energy strength observed in charged systems. However, if we rearrange Figure 2, grouping the complexes according to the ring structure of the double hydrogen bond, we can shed some light on the nature of their stability. In Figure 3, we have plotted the interaction energy components according to the topology of the ring structure formed due to a double hydrogen bond with an exception of charged species which are the first group. An inspection of Figure 3 indicates that we observe very similar interactions in the complexes characterized by the same or similar hydrogen-bond "ring structure". This is also reflected by the local nature of interaction induced electron density deformation observed in Figures 4−7 and the results of AIM analysis. Another important conclusion is also the fact that in the case of all of the studied neutral complexes the most important component of the interaction energy is in fact the delocalization term which contributes almost half of the total interaction energy.

A very important aspect, hardly touched in the preceding paragraphs, is the reliability of the theoretical model adopted in the present study. As far as MP2 interaction energies are concerned, they can be compared to more accurate electron correlation treatments like CCSD or CCSD(T). The data presented in Tables 2−4 show that the average differences between MP2/aug-cc-pVDZ and CCSD/aug-cc-pVDZ interaction energies do not exceed 1 kcal/mol and are 0.7, 0.4, and 0.4 kcal/mol for complexes with adenine, cytosine, and uracil, respectively. For the two complexes, denoted as (o) and (q), we have also computed interaction energies at the CCSD(T)/aug-cc-pVDZ level of theory. The differences, $\Delta E^{CCSD(T)} - \Delta E^{MP2}$, were quite insignificant: −0.01 and 0.09 kcal/mol,

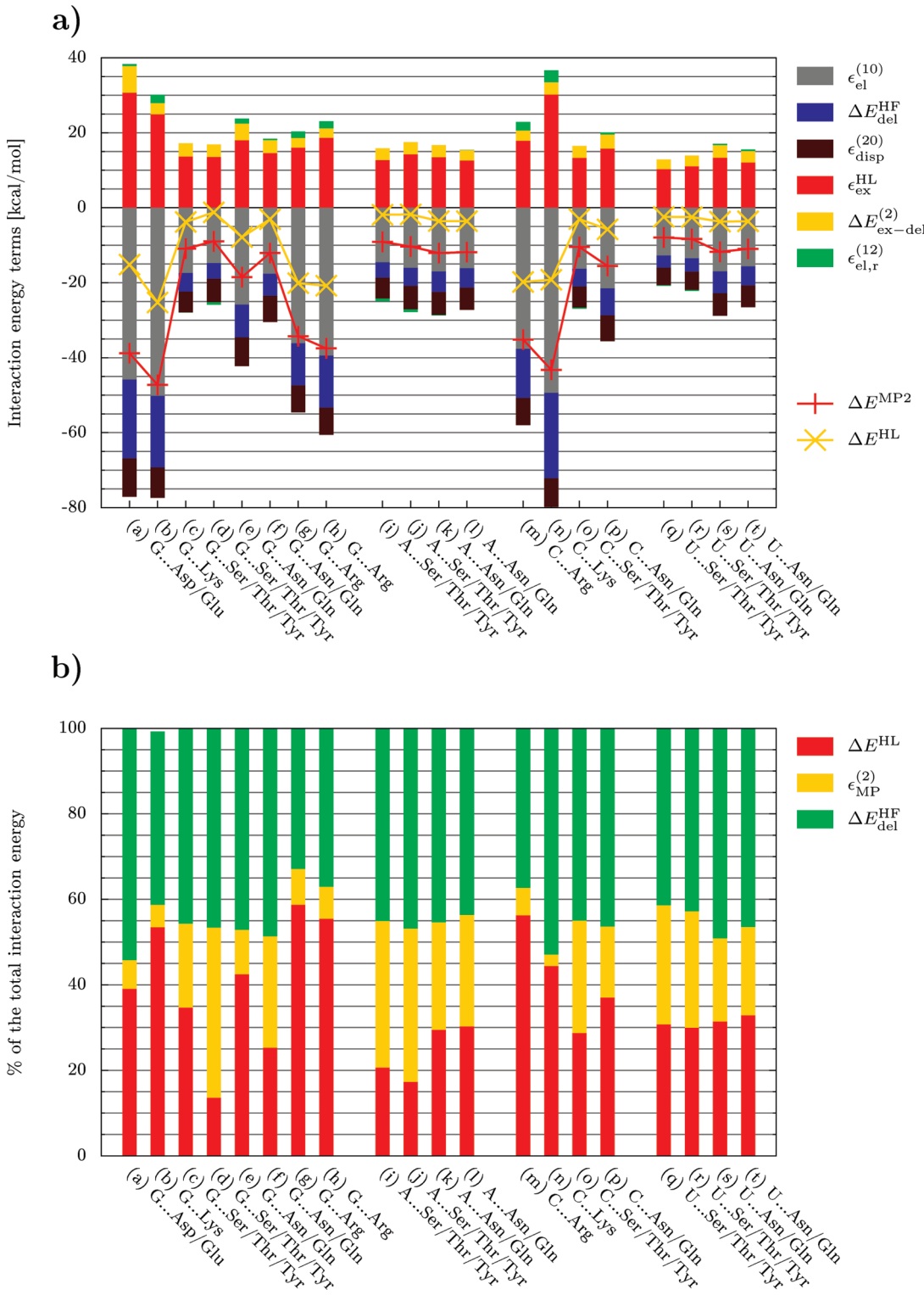

Figure 2. Intermolecular interaction energy and its components for complexes of nucleic acid bases and amino acid side chains (a) and the respective relative contributions of the Heitler−London, delocalization, and correlation interaction energy components (b). Complexes are ordered according to the constituent nucleic acid base.

respectively. The basis set used in the present study is also quite reliable for this type of calculations. For the complex denoted as (n), the values of MP2 intermolecular interaction energies are −43.24, −44.58, and −44.40 kcal/mol for the aug-cc-pVDZ, cc-pVTZ, and aug-cc-pVTZ basis set, respectively. In summary, we find that the MP2/aug-cc-pVDZ level of theory is a very reasonable compromise between efficiency and accuracy for the considered set of complexes. Similar observations concerning the accuracy of the MP2 method have already been reported by Berka et al. for amino acid pairs.[42]

Application of the QTAIM to the discussed complexes allowed us to observe two hydrogen-bond critical points (HBCPs) between nucleic acid bases and amino acid side chains for all complexes but C···Lys denoted as (n), in which case only one hydrogen-bond path was found. The values of electron density, $\rho(\mathbf{r}_{BCP})$, its Laplacian, $\nabla^2\rho(\mathbf{r}_{BCP})$, as well as electronic

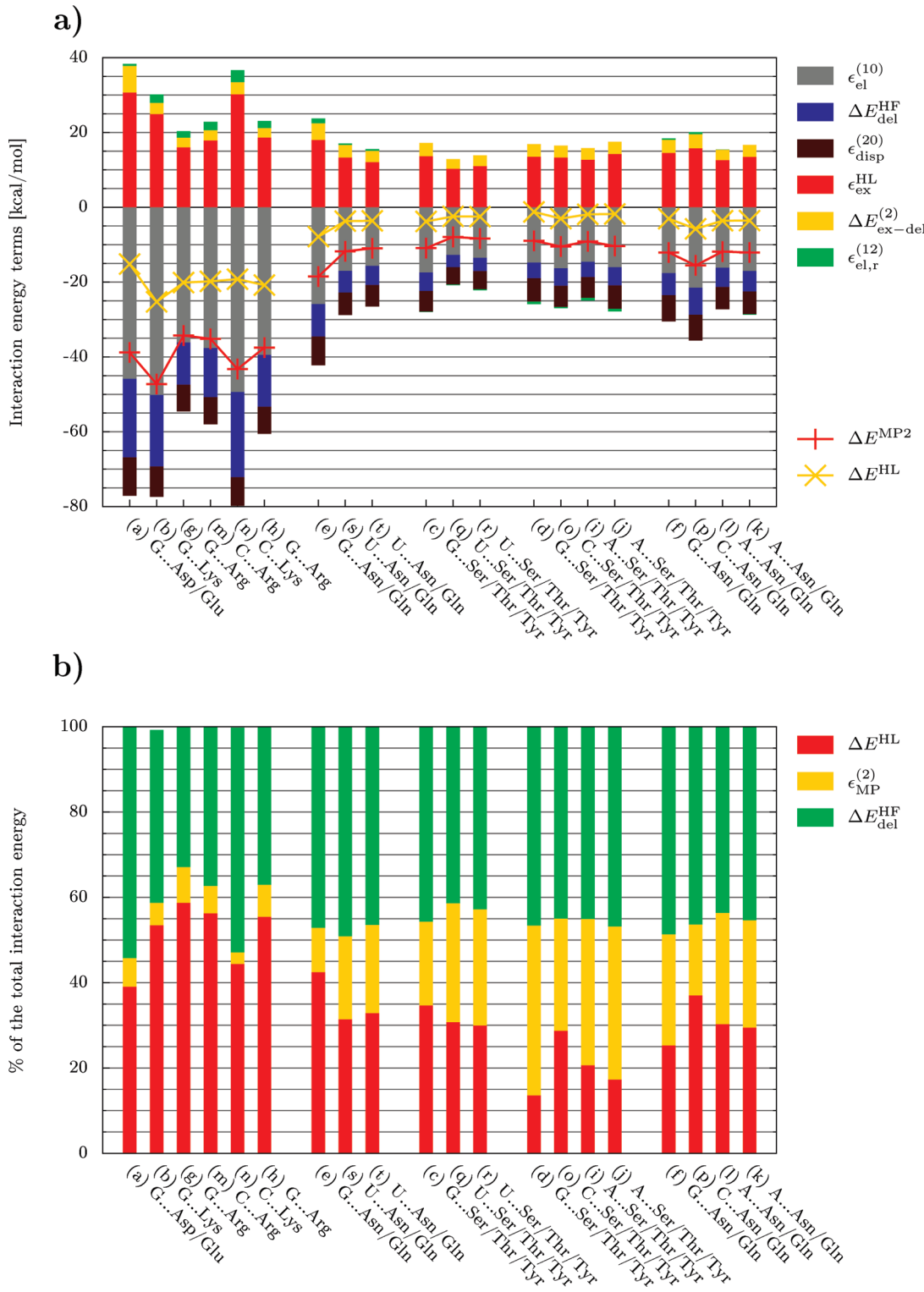

Figure 3. Intermolecular interaction energy and its components for complexes of nucleic acid bases and amino acid residues (a) and the respective relative contributions of the Heitler−London, delocalization, and correlation interaction energy components (b). Complexes are ordered according to the ring structure of the double hydrogen bond.

energy density, $H(\mathbf{r}_{BCP})$, electronic kinetic energy density, $G(\mathbf{r}_{BCP})$, and electronic potential energy density, $V(\mathbf{r}_{BCP})$, at the HBCPs, calculated at the MP2/aug-cc-pVDZ and HF/aug-cc-pVDZ levels of theory are listed in Table 5. One can see that all electron densities and Laplacian values at the HBCPs are well within the range suggested for H-bonds by Koch and Popelier[43] (i.e., 0.002−0.034 au for electron densities and 0.024−0.139 au for Laplacian). It is well established that the magnitude of the $\rho(\mathbf{r}_{BCP})$ at the HBCP can reflect the strength of the hydrogen bond.[44] In Figure 8, we have plotted the magnitudes of the interaction energy and its components against the sum of electron densities at the HBCPs. For correlation with the first-order electrostatic, Heitler−London exchange, and delocalization terms, we have adopted the HF densities, whereas in the case of the total interaction energies and electron correlation corrections we have used the generalized MP2 densities. The plot of the total interaction energy shown in Figure 8 clearly distinguishes among two sets of compounds: charged

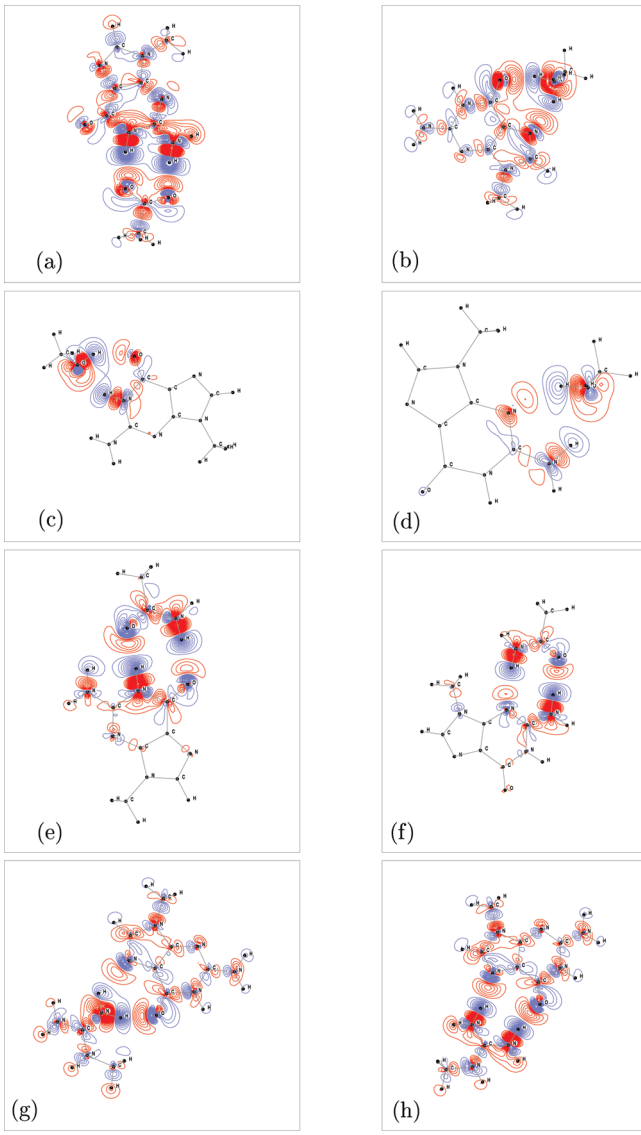

Figure 4. Interaction difference density maps for guanine−amino acid side-chain complexes.

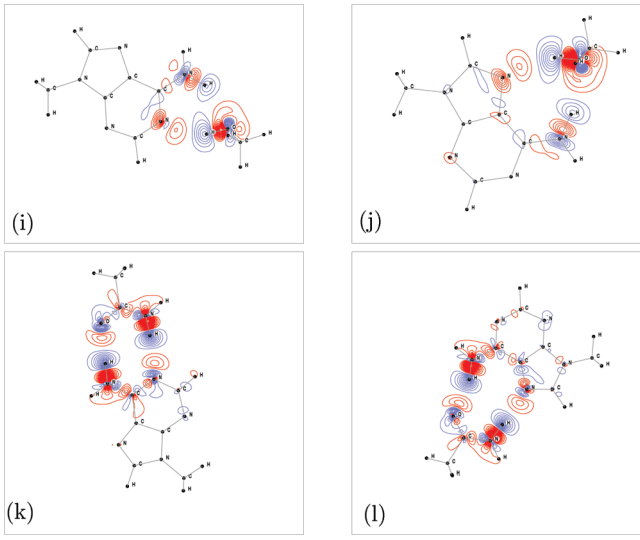

Figure 5. Interaction difference density maps for adenine−amino acid side-chain complexes.

and neutral species. The relationships for both sets have a linear character, and the least-squares fitting curves are almost parallel

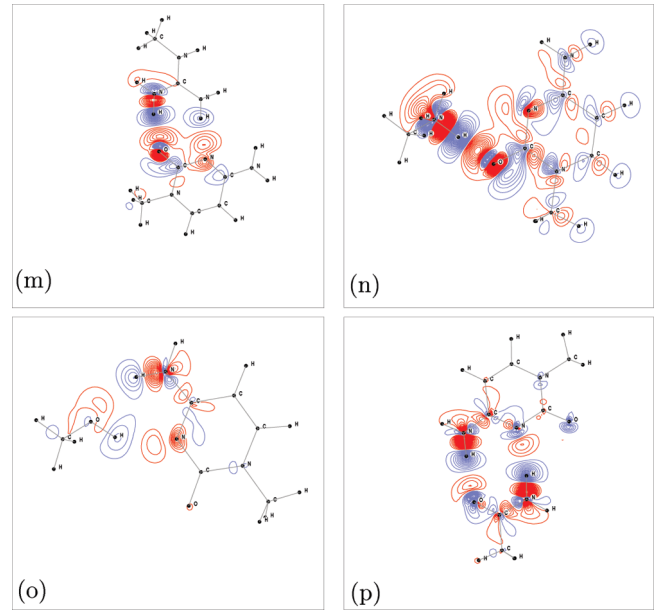

Figure 6. Interaction difference density maps for cytosine−amino acid side-chain complexes.

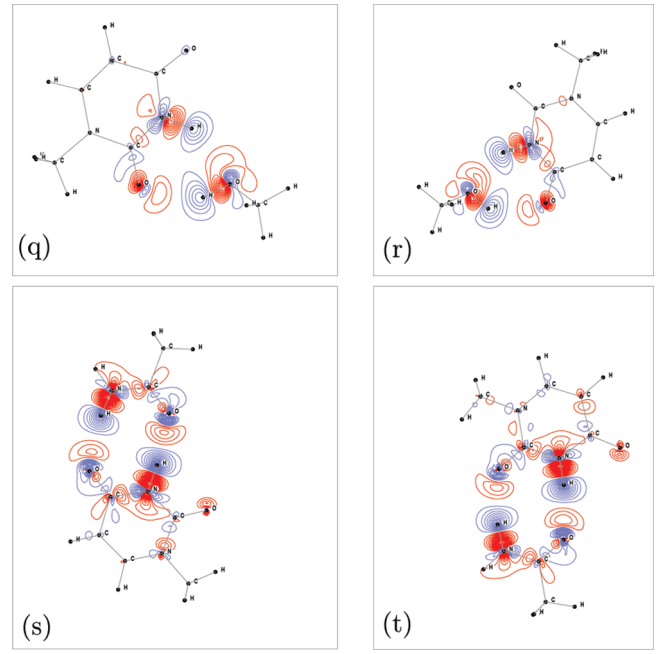

Figure 7. Interaction difference density maps for uracil−amino acid side-chain complexes.

with the energies of charged species shifted by about 15 kcal/mol with respect to the neutral ones. Judging by the plots of $\Delta E_{\mathrm{del}}^{\mathrm{HF}}$ and $\epsilon_{\mathrm{el}}^{(10)}$, this shift can be attributed mainly to the electrostatic interactions and to some extent also to the mutual polarization. It is interesting to note that it seems that the first-order electrostatic interaction energy grows slightly faster with the $\rho(\mathbf{r}_{\mathrm{HBCP}})$ in the case of neutral species, whereas the delocalization term grows faster for the charged complexes. In the case of the exchange effects, both trends virtually coincide. We did not observe a statistically important correlation of $\epsilon_{\mathrm{MP}}^{(2)}$ or its components with densities at HBCPs.

As a result of the double-hydrogen-bond character of interactions in a vast majority of the investigated systems, one observes formation of a ring critical point (RCP). The RCP is the point of the minimum electron density within the ring surface and a

TABLE 5: Topological Properties (Given in au) of the Hydrogen-Bond Critical Points for the Systems Analyzed Here[a]

		HF/aug-cc-pVDZ					MP2/aug-cc-pVDZ				
complex	HB	$\rho(\mathbf{r}_{BCP})$	$\nabla^2\rho(\mathbf{r}_{BCP})$	$G(\mathbf{r}_{BCP})$	$V(\mathbf{r}_{BCP})$	$H(\mathbf{r}_{BCP})$	$\rho(\mathbf{r}_{BCP})$	$\nabla^2\rho(\mathbf{r}_{BCP})$	$G(\mathbf{r}_{BCP})$	$V(\mathbf{r}_{BCP})$	$H(\mathbf{r}_{BCP})$
G···Asp/Glu (a)	1	0.02943	0.11230	0.02568	−0.02329	0.00240	0.03179	0.10113	0.02483	−0.02438	0.00045
	2	0.03642	0.13468	0.03230	−0.03092	0.00137	0.03913	0.12034	0.03102	−0.03196	−0.00094
G···Lys (b)	1	0.02598	0.08483	0.01955	−0.01789	0.00166	0.02752	0.07642	0.01878	−0.01846	0.00032
	2	0.03699	0.14109	0.03357	−0.03186	0.00170	0.03929	0.12844	0.03245	−0.03279	−0.00034
G···Ser/Thr/Tyr (c)	1	0.02028	0.07234	0.01722	−0.01635	0.00087	0.02194	0.06630	0.01690	−0.01723	−0.00033
	2	0.02105	0.07932	0.01804	−0.01625	0.00179	0.02288	0.07313	0.01784	−0.01740	0.00044
G···Ser/Thr/Tyr (d)	1	0.02161	0.07368	0.01663	−0.01485	0.00179	0.02323	0.06685	0.01621	−0.01572	0.00050
	2	0.01735	0.06098	0.01432	−0.01339	0.00093	0.01887	0.05670	0.01423	−0.01428	−0.00005
G···Asp/Gln (e)	1	0.01925	0.07084	0.01590	−0.01410	0.00181	0.02089	0.06466	0.01562	−0.01507	0.00055
	2	0.02818	0.11025	0.02493	−0.02230	0.00263	0.03045	0.09969	0.02422	−0.02352	0.00070
G···Asp/Gln (f)	1	0.01694	0.05332	0.01194	−0.01055	0.00139	0.01824	0.04832	0.01164	−0.01121	0.00044
	2	0.02329	0.09137	0.02024	−0.01764	0.00260	0.02516	0.08345	0.01980	−0.01873	0.00106
G···Arg (g)	1	0.01435	0.04580	0.01072	−0.00999	0.00073	0.01529	0.04248	0.01045	−0.01028	0.00017
	2	0.03028	0.12145	0.02763	−0.02491	0.00273	0.03237	0.11060	0.02677	−0.02589	0.00088
G···Arg (h)	1	0.02251	0.07563	0.01667	−0.01444	0.00224	0.02409	0.06753	0.01600	−0.01512	0.00088
	2	0.02951	0.12579	0.02794	−0.02443	0.00351	0.03156	0.11589	0.02724	−0.02552	0.00173
A···Ser/Thr/Tyr (i)	1	0.01562	0.05493	0.01289	−0.01205	0.00084	0.01700	0.05140	0.01284	−0.01282	0.00001
	2	0.02131	0.07188	0.01615	−0.01433	0.00182	0.02291	0.05400	0.01571	−0.01516	0.00054
A···Ser/Thr/Tyr (j)	1	0.01942	0.06919	0.01594	−0.01458	0.00136	0.02117	0.06338	0.01575	−0.01566	0.00009
	2	0.02178	0.07698	0.01694	−0.01464	0.00230	0.02338	0.06970	0.01647	−0.01551	0.00096
A···Asn/Gln (k)	1	0.02009	0.07667	0.01700	−0.01483	0.00217	0.02180	0.07007	0.01669	−0.01586	0.00083
	2	0.01821	0.05755	0.01284	−0.01130	0.00155	0.01957	0.05185	0.01246	−0.01196	0.00050
A···Asp/Gln (l)	1	0.01724	0.05574	0.01235	−0.01076	0.00159	0.01855	0.05046	0.01202	−0.01143	0.00059
	2	0.02037	0.08088	0.01779	−0.01535	0.00243	0.02203	0.07448	0.01750	−0.01638	0.00112
C···Arg (m)	1	0.01809	0.05851	0.01290	−0.01117	0.00173	0.01953	0.05302	0.01259	−0.01192	0.00067
	2	0.03024	0.12837	0.02868	−0.02527	0.00341	0.03230	0.11852	0.02801	−0.02638	0.00163
C···Lys (n)	1	0.06249	0.18405	0.05732	−0.06862	−0.01131	0.06590	0.16716	0.05557	−0.06935	−0.01378
C···Ser/Thr/Tyr (o)	1	0.01609	0.05728	0.01332	−0.01232	0.00100	0.01757	0.05358	0.01328	−0.01316	0.00012
	2	0.02195	0.07486	0.01689	−0.01506	0.00183	0.02348	0.06804	0.01641	−0.01581	0.00078
C···Asp/Gln (p)	1	0.02157	0.08338	0.01845	−0.01606	0.00239	0.02338	0.07621	0.01809	−0.01713	0.00096
	2	0.02043	0.06790	0.01498	−0.01298	0.00200	0.02185	0.06157	0.01455	−0.01371	0.00084
U···Ser/Thr/Tyr (q)	1	0.01594	0.05710	0.01325	−0.01222	0.00103	0.01737	0.05351	0.01322	−0.01307	0.00015
	2	0.01925	0.07116	0.01671	−0.01562	0.00108	0.02072	0.06596	0.01647	−0.01646	0.00002
C···Ser/Thr/Tyr (r)	1	0.01671	0.05797	0.01406	−0.01364	0.00043	0.01812	0.05386	0.01391	−0.01436	−0.00045
	2	0.01982	0.07349	0.01682	−0.01526	0.00156	0.02150	0.06802	0.01664	−0.01627	0.00036
U···Asn/Gln (s)	1	0.01761	0.06642	0.01481	−0.01301	0.00180	0.01912	0.06147	0.01466	−0.01395	0.00071
	2	0.02295	0.09022	0.01989	−0.01723	0.00266	0.02490	0.08238	0.01948	−0.01835	0.00112
C···Asn/Gln (t)	1	0.02000	0.07698	0.01697	−0.01469	0.00228	0.02177	0.07062	0.01671	−0.01576	0.00095
	2	0.01820	0.07146	0.01575	−0.01364	0.00211	0.01964	0.06659	0.01562	−0.01459	0.00103

[a] The second column refers to the hydrogen bonds for complexes shown in Figure 1. We use the following scheme for labeling: the left or upper hydrogen bonds are denoted as 1, while the lower or right hydrogen bonds are labeled as 2.

maximum on the ring line.[45] To the best of our knowledge, there were only a few studies devoted to a systematic analysis of electron density at RCP. It has been shown by Grabowski et al. that the electron density at RCP correlates well with the traditional descriptors of the hydrogen-bond strength such as electron density or electronic potential energy density at HBCP.[46,47] In the case of complexes analyzed here, no such correlations could be found (see Figure 9). The lack of such a correlation could be explained by a relatively wide set of heterogeneous complexes analyzed here in contrast to the previous studies.

A careful analysis of the results reported in Table 5 allows us to conclude that the vast majority of the hydrogen bonds analyzed here have a closed-shell nature of interactions. It can be confirmed by positive values of both the Laplacian and the electronic energy density at the HBCPs.[48] Some authors claim that if the Laplacian is positive and $H(\mathbf{r}_{BCP})$ is negative, then the interactions are partly covalent in nature.[49] Such a situation occurs in the complexes of guanine with Asp/Glu, Lys, Ser/Thr/Tyr (a−d), the complex of cytosine and lysine (n), as well as the dimer of uracil and Ser/Thr/Tyr (r) for which we have obtained the negative values of $H(\mathbf{r}_{BCP})$ using generalized MP2 densities. However, in most of the aforementioned complexes, these values are very close to zero, ranging from −0.00005 to −0.00094 au with the possible exception of cytosine and lysine complex (n), for which $H(\mathbf{r}_{BCP})$ equals −0.01378 au. Grabowski et al. suggested that for the hydrogen bonds which are at least partially covalent ($\nabla^2\rho(\mathbf{r}_{BCP}) > 0$ and $H(\mathbf{r}_{BCP}) < 0$), the ratio of ΔE_{del}^{HF} and $\epsilon_{el}^{(10)}$ should be greater than 0.45. In the case of aforementioned complex (n), such a condition is fulfilled, since $\Delta E_{del}^{HF}/\epsilon_{el}^{(10)} = 0.46$.

Conclusions

In this study, 20 nucleic acid base−amino acid side-chain complexes have been analyzed with an emphasis put on the nature of intermolecular interactions in these systems. In the case of the set comprised of the neutral amino acid side chains, we have observed a predominant role of the delocalization component in stabilization of the complexes, indicating a significant mutual polarization of the interacting species. The remaining systems, containing positively and negatively charged amino acid side chains, are stabilized to a large extent due to the Heitler−London component of the interaction energy. What we also observed is that the dispersion contribution, although much smaller in magnitude than delocalization and electrostatic

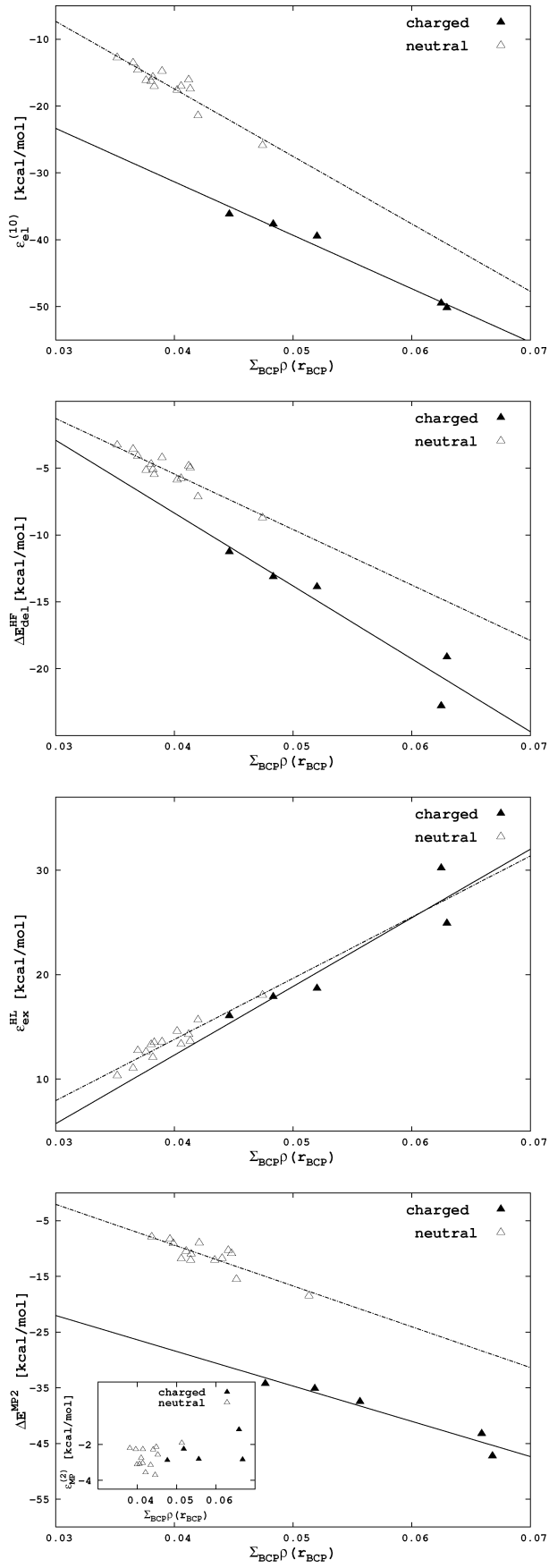

Figure 8. Dependence of the intermolecular interaction energy and its components on the sum of electron densities at the hydrogen-bond critical points (BCPs) for the studied systems. All calculations were performed using the aug-cc-pVDZ basis set. See text for details.

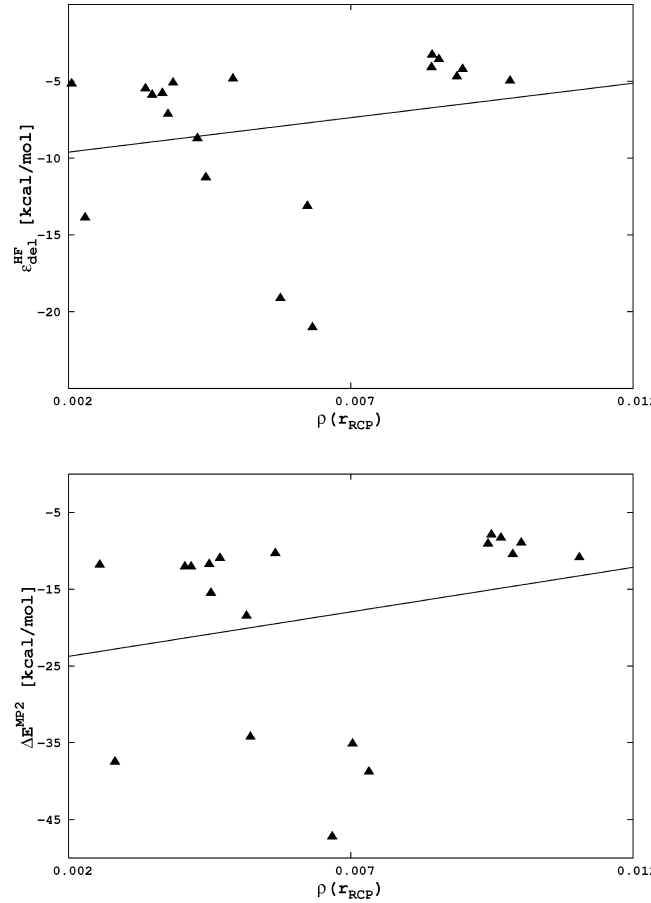

Figure 9. Dependence of the total MP2 intermolecular interaction energy and the delocalization component on the electron density at the ring critical point (RCP) for the studied systems. All calculations were performed using the aug-cc-pVDZ basis set. See text for details.

contributions, might still be quite significant for certain complexes. For the two considered sets of complexes, namely, containing positively charged and neutral amino acid side chains, a good correlation between the sum of densities in hydrogen-bond critical points and the Hartree−Fock intermolecular interaction energy components has been observed. Unfortunately, a similarly good correlation has not been observed between the ring critical point properties and any of the analyzed interaction energy components. Another important finding of this study is that the changes of electronic densities upon formation of neutral complexes are local in their nature and mainly concern the regions involved in hydrogen bonding. The observed locality of intermolecular interaction in neutral complexes might have a significant impact on the molecular recognition processes. This, however, needs further analysis.

Acknowledgment. This work was supported by computational grants from Wroclaw Center for Networking and Supercomputing (WCSS). The allocation of computing time is greatly appreciated.

References and Notes

(1) Seeman, N. C.; Rosenberg, J. M.; Rich, A. *Proc. Natl. Acad. Sci. U.S.A.* **1976**, *73*, 804–808.

(2) Jones, S.; van Heyningen, P.; Berman, H. M.; Thornton, J. M. *J. Mol. Biol.* **1999**, *287*, 877–896.

(3) Sathyapriya, R.; Vishveshwara, S. *Nucleic Acids Res.* **2004**, *32*, 4109–4118.

(4) Lejeune, D.; Delsaux, N.; Charloteaux, B.; Thomas, A.; Brasseur, R. *Proteins: Struct., Funct., Bioinform.* **2005**, *61*, 258–271.

(5) Gromiha, M. M.; Siebers, J. G.; Selvaraj, S.; Kono, H.; Sarai, A. *J. Mol. Biol.* **2004**, *337*, 285–294.
(6) Paillard, G.; Lavery, R. *Structure* **2004**, *12*, 113–122.
(7) Pabo, C. O.; Sauer, R. T. *Annu. Rev. Biochem.* **1984**, *53*, 293–321.
(8) Mukherjee, S.; Majumdar, S.; Bhattacharyya, D. *J. Phys. Chem. B* **2005**, *109*, 10484–10492.
(9) Ellis, J. J.; Broom, M.; Jones, S. *Proteins: Struct., Funct., Bioinform.* **2007**, *66*, 903–911.
(10) Jeong, E.; Kim, H.; Lee, S.-W.; Han, K. *Mol. Cells* **2003**, *16*, 161–167.
(11) Shulman-Peleg, A.; Shatsky, M.; Nussinov, R.; Wolfson, H. J. *J. Mol. Biol.* **2008**, *379*, 299–316.
(12) Cheng, A. C.; Chen, W. W.; Fuhrmann, C. N.; Frankel, A. D. *J. Mol. Biol.* **2003**, *327*, 781–796.
(13) Cheng, A. C.; Frankel, A. D. *J. Am. Chem. Soc.* **2004**, *126*, 434–435.
(14) Rutledge, L. R.; Wetmore, S. D. *J. Chem. Theory Comput.* **2008**, *4*, 1768–1780.
(15) Rutledge, L. R.; Durst, H. F.; Wetmore, S. D. *Phys. Chem. Chem. Phys.* **2008**, *10*, 2801–2812.
(16) Gu, J.; Wang, J.; Leszczynski, J. *J. Phys. Chem. B* **2006**, *110*, 13590–13596.
(17) Gutowski, M.; Piela, L. *Mol. Phys.* **1988**, *64*, 337.
(18) Frey, R. F.; Davidson, E. R. *J. Chem. Phys.* **1989**, *90*, 5555.
(19) Kitaura, K.; Morokuma, K. *Int. J. Quantum Chem.* **1976**, *10*, 325–340.
(20) Werner, H. J.; et al. *MOLPRO*, version 2006.1.
(21) Schmidt, M. W.; Baldridge, K. K.; Boatz, J. A.; Elbert, S. T.; Gordon, M. S.; Jensen, J. H.; Koseki, S.; Matsunaga, N.; Nguyen, K. A.; Su, S. J.; Windus, T. L.; Dupuis, M.; Montgomery, J. A. *J. Comput. Chem.* **1993**, *14*, 1347.
(22) Gora, R. W. *EDS package*, revision 2.8.1; Wrocław, Poland, 1998−2008.
(23) Gutowski, M.; Duijneveldt, F. B.; Chałasiński, G.; Piela, L. *Mol. Phys.* **1987**, *61*, 223.
(24) Sokalski, W. A.; Roszak, S.; Pecul, K. *Chem. Phys. Lett.* **1988**, *153*, 153.
(25) Chałasiński, G.; Szczęśniak, M. M. *Mol. Phys.* **1988**, *63*, 205.
(26) Cybulski, S. M.; Chałasiński, G.; Moszyński, R. *J. Chem. Phys.* **1990**, *92*, 4357.
(27) Chałasiński, G.; Szczęśniak, M. M. *Chem. Rev.* **1994**, *94*, 1723.
(28) Hirschfelder, J. *Chem. Phys. Lett.* **1967**, *1*, 325.
(29) Moszyński, R.; Rybak, S.; Cybulski, S.; Chałasiński, G. *Chem. Phys. Lett.* **1990**, *166*, 609.
(30) Boys, S. F.; Bernardi, F. *Mol. Phys.* **1970**, *19*, 553.
(31) Gora, R. W.; Bartkowiak, W.; Roszak, S.; Leszczynski, J. *J. Chem. Phys.* **2002**, *117*, 1031.
(32) Gora, R. W.; Bartkowiak, W.; Roszak, S.; Leszczynski, J. *J. Chem. Phys.* **2004**, *120*, 2802.
(33) Gora, R. W.; Sokalski, W. A.; Leszczynski, J.; Pett, V. B. *J. Phys. Chem. B* **2005**, *109*, 2027.
(34) Gora, R. W. *DENDIF package*, revision 2.1.2; Wrocław, Poland, 2001.
(35) Schaftenaar, G.; Noordik, J. H. *J. Comput.-Aided Mol. Des.* **2000**, *14*, 123.
(36) Bader, R. F. W. *Atoms In Molecules, A Quantum Theory*; Oxford University Press: Oxford, U.K., 1990.
(37) Bader, R. F. W. *Chem. Rev.* **1991**, *91*, 893.
(38) Handy, N. C.; H. F. S. *J. Chem. Phys.* **1984**, *81*, 5031–5033.
(39) Bader, R. F. W.; MacDougall, P. J.; Lau, C. D. H. *J. Am. Chem. Soc.* **1984**, *106*, 1594.
(40) Biegler-Konig, F. *AIM2000 package*; University of Applied Sciences: Bielefeld, Germany.
(41) Fersht, A. R.; Shi, J. P.; Knill-Jones, J.; Lowe, D. M.; Wilkinson, A. J.; Blow, D. M.; Brick, P.; Carter, P.; Waye, M. M. Y.; Winter, G. *Nature* **1985**, *314*, 235–238.
(42) Berka, K.; Laskowski, R.; Rilley, K. E.; Hobza, P.; Vondrasek, J. *J. Chem. Theory Comput.* **2009**, *5*, 982–992.
(43) Koch, U.; Popelier, P. L. A. *J. Phys. Chem.* **1995**, *99*, 9747.
(44) Grabowski, S. J. *J. Phys. Chem. A* **2000**, *104*, 5551.
(45) Popelier, P. *Atoms in Molecules, An Introduction*; Pearson Education Ltd: Prentice Hall, NJ, 2000.
(46) Grabowski, S. J. *Monatsch. Chem.* **2002**, *133*, 1373.
(47) Wojtulewski, S.; Grabowski, S. J. *Chem. Phys. Lett.* **2003**, *378*, 388.
(48) Cremer, D.; Kraka, E. *Angew. Chem., Int. Ed.* **1984**, *23*, 637.
(49) Arnold, W. D.; Oldfield, E. *J. Am. Chem. Soc.* **2000**, *122*, 12835.

JP904146M